Received: 28 April 2017 | Revised: 28 February 2018 | Accepted: 6 March 2018

DOI: 10.1111/pce.13198

ORIGINAL ARTICLE

WILEY Plant, Cell & Environment

Is desiccation tolerance and avoidance reflected in xylem and phloem anatomy of two coexisting arid-zone coniferous trees?

Sanna Sevanto[1] | Max Ryan[1] | L. Turin Dickman[1] | Dominique Derome[2] | Alessandra Patera[3,4] | Thijs Defraeye[2,5] | Robert E. Pangle[6] | Patrick J. Hudson[6] | William T. Pockman[6]

[1] Earth and Environmental Sciences Division, Los Alamos National Laboratory, Bikini Atoll Road MS J535, Los Alamos, NM, 87545, USA

[2] Laboratory for Multiscale Studies in Building Physics, Swiss Federal Laboratories for Material Science and Technology (Empa), Ueberlandstrasse 129, 8600 Duebendorf, Switzerland

[3] Swiss Light Source, Paul Scherrer Institute, 5232 Villigen, Switzerland

[4] Centre d'Imagerie BioMedicale, Ecole Polytechnique Federale de Lausanne, 1015 Lausanne, Switzerland

[5] Chair of Building Physics, ETH Zurich, Stefano-Franscini-Platz 5, 8093 Zurich, Switzerland

[6] Department of Biology, University of New Mexico, Castetter Hall 1480, Yale Boulevard NE, Albuquerque, NM, 87131, USA

Correspondence
S. Sevanto, Los Alamos National Laboratory, Bikini Atoll Rd. MS J495, Los Alamos, NM 87545, USA.
Email: sanna@lanl.gov

Funding information
UNM Sevilleta Field Station, and Paul Scherrer Institute, Grant/Award Number: 20120914; Department of Energy's Office of Science (BER); Sevilleta LTER, Grant/Award Number: NSF DEB-0620482; Los Alamos National Laboratory LDRD, Grant/Award Numbers: 20160373ER and 20130442ER

Abstract

Plants close their stomata during drought to avoid excessive water loss, but species differ in respect to the drought severity at which stomata close. The stomatal closure point is related to xylem anatomy and vulnerability to embolism, but it also has implications for phloem transport and possibly phloem anatomy to allow sugar transport at low water potentials. Desiccation-tolerant plants that close their stomata at severe drought should have smaller xylem conduits and/or fewer and smaller interconduit pits to reduce vulnerability to embolism but more phloem tissue and larger phloem conduits compared with plants that avoid desiccation. These anatomical differences could be expected to increase in response to long-term reduction in precipitation. To test these hypotheses, we used tridimensional synchroton X-ray microtomograph and light microscope imaging of combined xylem and phloem tissues of 2 coniferous species: one-seed juniper (*Juniperus monosperma*) and piñon pine (*Pinus edulis*) subjected to precipitation manipulation treatments. These species show different xylem vulnerability to embolism, contrasting desiccation tolerance, and stomatal closure points. Our results support the hypothesis that desiccation tolerant plants require higher phloem transport capacity than desiccation avoiding plants, but this can be gained through various anatomical adaptations in addition to changing conduit or tissue size.

KEYWORDS

conduit size, interconduit pit, phloem transport, stomatal closure point, synchrotron X-ray microtomography, xylem vulnerability

1 | INTRODUCTION

One key feature of plant life is the need to take up CO_2 from the atmosphere for photosynthesis but control simultaneous water loss that occurs through the stomata. Water uptake from the soil is usually slower than transpiration from the leaves when stomata are open. This leads to decreasing water reserves and increasing water tension in the stem during the day (Irvine & Grace, 1997; Sevanto et al., 2005). Increasing water tension can lead to embolization of xylem conduits (Tyree & Sperry, 1989). If uncontrolled and excessive, embolism can spread and lead to catastrophic failure of the water conducting system (Sperry & Pockman, 1993). Therefore, in some conditions, it is preferable for the plant to close the stomata to avoid water loss, even if this means simultaneously blocking CO_2 uptake for photosynthesis.

The conditions considered severe enough to favor stomatal closure differ between plants even in the same environment (Brodribb, Holbrook, Edwards, & Gutierrez, 2003; Quero, Sterck, Martinez-Vilalta, & Villar, 2011). Desiccation-avoiding (isohydric) plants close their stomata at relatively high tissue water potentials (low water

stress), relying on their carbon reserves for the duration of drought. Desiccation-tolerant (anisohydric) plants keep the stomata open longer during drought (Tardieu & Simonneau, 1998), maintaining a more positive carbon balance (McDowell et al., 2008). In recent years, theories for explaining these differences have been developed and tested to allow improved prediction of plant responses to changing environment (Berninger, Mäkelä, & Hari, 1996; Cowan & Farquhar, 1977; Katul, Manzoni, Palmroth, & Oren, 2010; Manzoni et al., 2013; Meinzer, 2002; Sperry et al., 2016). These theories state that to avoid catastrophic hydraulic failure, the stomatal closure point (leaf water potential at which stomata close during drought) is linked with xylem vulnerability to embolism (Sperry, 1986; Cochard, Breda, & Granier, 1996; Nardini & Salleo, 2000; Sperry, 2000; Brodribb et al., 2003; Brodribb, 2009). Plants that tend to have a more vulnerable xylem close their stomata earlier during drought than plants that have more embolism-resistant xylem (Meinzer, Johnson, Lachenbruch, McCulloh, & Woodruff, 2009).

Xylem vulnerability to embolism has been linked with several anatomical features. Generally, large and long conduits that provide a high hydraulic conductivity are more vulnerable to embolism than short and narrow conduits (Gleason et al., 2015). This has been observed both between (e.g., Scoffoni et al., 2017; Smith, Fridley, Yin, & Bauerle, 2013) and within species (Cai & Tyree, 2010) and even between different tissues in an individual (Domec & Gartner, 2002; LoGullo, Salleo, Piaceri, & Rosso, 1995). Highly conductive xylem could give a plant a competitive advantage (Brodribb & Hill, 1999). But because of the increased vulnerability, a trade-off between hydraulic conductivity and xylem vulnerability favors small conduits in arid environments (Martinez-Vilalta et al., 2002; Brodersen, 2015; but see also Gleason et al., 2015). Whether the vulnerability of large conduits is purely due to large conduit volume leading to a large amount of dissolved gases that could increase the probability of bubble formation (Sevanto, Holbrook, & Ball, 2012) or some other factor that correlates with conduit volume, such as number of pits, total pit area (Wheeler, Sperry, Hacke, & Hoang, 2005), pit structure (Choat, Ball, Luly, & Holtum, 2003; Choat, Jansen, Zwieniecki, Smets, & Holbrook, 2004), or size of largest interconduit pores (Christman, Sperry, & Adler, 2009) is still unclear. For conifers, there is increasing evidence that drought-induced embolism is related to the anatomy of pit structures and interconduit pore size (Brodersen, Jansen, Choat, Rico, & Pittermann, 2014; Cochard, Hölttä, Herbette, Delzon, & Mencuccini, 2009; Delzon, Douthe, Sala, & Cochard, 2010; Jansen et al., 2012; Pittermann et al., 2010; Wheeler et al., 2005) with air seeding thought to be the main mechanisms of bubble formation (Cochard et al., 2009; Hacke, Sperry, & Pittermann, 2004). High pit abundance and/or large pit size, while reducing flow resistance in the xylem, could lead to high vulnerability by creating more "weak spots" at the cell walls (Wheeler et al., 2005).

In addition to the xylem, the plant hydraulic system includes the sugar transporting phloem. Phloem and xylem are located next to each other, and they generally operate at hydraulic equilibrium (Thompson & Holbrook, 2003). When xylem tension increases because of increased transpiration, phloem water potential quickly adjusts osmotically to match that of the adjacent xylem to avoid water leakage to the xylem and possible loss of turgor in phloem cells (for review, see Savage et al., 2016). The good hydraulic connection between the xylem and the phloem has led to theories on how limitations in phloem function could lead to stomatal closure (Nikinmaa et al., 2013) or even plant mortality during drought (McDowell & Sevanto, 2010; Sala, Piper, & Hoch, 2010). If phloem transport capacity is compromised by an increase in viscosity of the phloem sap resulting from osmoregulation to balance water potential with the xylem, then increasing sugar concentration in the leaves could induce stomatal closure (Hölttä, Mencuccini, & Nikinmaa, 2009; Nikinmaa et al., 2013). On the other hand, if the osmoregulation fails due to declining carbohydrate reserves, phloem might lose turgor and collapse, facilitating plant mortality (Sevanto, 2014; Sevanto, McDowell, Dickman, Pangle, & Pockman, 2014).

Phloem anatomy of many plants is poorly characterized, and considerations of possible impacts of phloem function on stomatal control and plant survival during drought are very recent. Therefore, little is known about how phloem function and vulnerability to drought is reflected in phloem anatomy. Theoretically, the link between phloem anatomy, transport capacity, and vulnerability to drought could be defined by the strength of the hydraulic connection between the conduits and their surroundings including the xylem (Sevanto, 2014). If hydraulic conductivity between these tissues is relatively low, the conduits operate fairly independently, and axial flow through each conduit should approximately follow the Hagen–Poiseuille equation. In this case, phloem transport capacity during drought can be limited by increasing sap viscosity, which results from the increased need of osmoregulation with declining xylem water potential. Plants that operate at low leaf water potentials could structurally compensate for this by increasing conduit diameter or by increasing the number of phloem conduits (Hölttä et al., 2009; Sevanto, 2014). The relative increase in conduit diameter required to maintain transport capacity unchanged under declining water potential can be calculated by combining the semiempirical equation of Morison (2002) for viscosity increase as a response to increasing sucrose concentration with the Van't Hoff equation for the relationship of solute concentration and osmotic potential. Using the Hagen–Poiseuille equation for calculating mass flux (see Supporting Information) results in

$$\frac{D_2}{D_1} = \sqrt[4]{e^{\frac{4.68 \cdot 0.956 \cdot \left(\frac{V\Psi}{RT}\right)}{1-0.956 \cdot \left(\frac{V\Psi}{RT}\right)}}} \quad (1)$$

where D_1 and D_2 are the initial and final conduit diameters, V is the molar volume of sucrose in water solution, here taken at 20 °C (Fucaloro, Pu, Cha, Williams, & Conrad, 2007), Ψ is the tissue water potential, R the gas constant, and T temperature (K). To maintain a constant mass flux despite increasing sap viscosity, phloem conduits should increase in diameter by a factor of 2 in plants operating at water potential <−5 MPa compared with plants that close stomata at water potential of ~−2 MPa (Figure S1a). Similarly, if the phloem mass flux was maintained solely by increasing the number of conduits of similar size, plants operating at minimum water potential <−5 MPa should have 10 times more phloem conduits than plants that close stomata at ~−2 MPa (Figure S1b). These values, however,

are hard to verify empirically, because they are influenced by the tissue age and sample location, as well as the leaf area supported by these tissues and the magnitude of the hydraulic conductivity between phloem conduits and their surroundings.

In conifers, the phloem tissue consists almost solely of conduits and their companion cells (Strasburger cells; Schulz, 1990), and the buffering impact of parenchyma cells surrounding phloem conduits is small, leaving phloem conduit water potential linked more directly with xylem water potential than in many angiosperm species. The relatively strong hydraulic coupling between the xylem and the phloem results in a strong influence of the conductive capacity of one tissue on the other, and structural investments that increase conductivity of one also improve conductivity of the other (Hölttä et al., 2009). According to a modeling study, at stomatal closure point ~-5 MPa and with hydraulic conductivity between these tissues ~10^{-13} m Pa^{-1} s^{-1}, the abundance of xylem to phloem conduits should scale as 6:1 assuming similar conduit size in both tissues. At minimum xylem water potentials of ~−2 MPa, the amounts of xylem and phloem conduits should scale roughly 22:1 (Hölttä et al., 2009). Thus, plants operating at low leaf water potentials should have relatively larger phloem to xylem ratios than plants that close stomata relatively early during drought.

Structurally, hydraulic coupling between the xylem and the phloem and between conduits within each tissue can be achieved either by interconduit pits (sieve pores in the phloem) or semipermeable conduit walls. In the first case, conduit walls can be impermeable to water and all water exchange between conduits occurs via the pits. This model matches the observations of xylem anatomy and flow (Kim, Park, & Hwang, 2014) and supports the use of Hagen–Poiseuille equation for describing the flow, even if the increased flow resistance in the pits introduces an offset from the theoretical maximum conductivity (Pittermann, Sperry, Hacke, Wheeler, & Sikkema, 2006). In the phloem, however, it is possible that the conduits are connected to their surroundings via semipermeable conduit walls facilitated, for example, by aquaporins (Laur & Hacke, 2014). In this case, a theory of flow in tubes with semipermeable walls is needed for the analysis (Sevanto, 2014). Fluid viscosity will not limit fluxes, because water exchange between the conduit and its surroundings constantly dilutes the solution. The mass flux also becomes directly proportional to the conduit radius (see e.g., Phillips & Dungan, 1993; Supporting Information), unlike in Hagen–Poiseuille flow where the flux is proportional to the fourth power of the conduit radius (Bird, Stweart, & Lightfoot, 2002; see also Supporting Information). This limits the capacity of the plant to increase tissue conductivity by adjustment of conduit size. The influence of increasing the number of conduits on tissue transport capacity is not as straight forward as in the case of conduits with nonpermeable walls because conduits would not operate as independent entities but more like an interconnected network.

Based on these considerations, we hypothesize that, in addition to a more embolism-resistant xylem, desiccation-tolerant plants that conduct photosynthesis and maintain phloem transport at low tissue water potentials should have a more conductive phloem than desiccation-avoiding plants. This high conductivity could be achieved by larger phloem conduits and/or larger phloem tissue (more conduits) if the phloem conduits are hydraulically relatively isolated from their surroundings. Alternatively, if the phloem conduits are hydraulically well connected to their surroundings, increased transport capacity could primarily be achieved via increased tissue size (more conduits) or increased hydraulic conductance between adjacent conduits. Similarly, if these traits are important for survival during drought, we would expect dry growth conditions to promote structural adaptation towards decreased vulnerability to embolism in the xylem in both plant groups and increased phloem transport capacity at high xylem water tensions in desiccation-tolerant species.

To test these hypotheses, we used phase contrast synchrotron X-ray microtomography imaging of xylem and phloem anatomy in piñon pine (*Pinus edulis*) and one-seed juniper (*Juniperus monosperma*) grown for 5 years under precipitation manipulation treatments(see e.g., Plaut et al., 2012). This method yields 3D datasets of the cellular structure in presence of water or sap allowing characterization of phloem geometry as it would be in situ. We also combine tomography with light microscopy to compare tissue size of the xylem and phloem. Piñon pine and one-seed juniper have been used in many studies as a model system of two coexisting species representing extremes of desiccation avoidance and tolerance (McDowell et al., 2008; Pangle et al., 2015; Plaut et al., 2012). Typical of pine trees, piñon pine closes its stomata at about −2.0 to −2.5 MPa leaf water potential, whereas the co-occurring one-seed juniper allows leaf water potential to drop to ~−5 MPa before stomatal closure (Garcia-Forner et al., 2016) maintaining photosynthesis rates up to 6 μmol m^{-2} s^{-1} at leaf water potentials below stomatal closure point of pine (Limousin et al., 2013). Piñon pine is also more vulnerable to xylem cavitation (P_{50} = −2.75 − −4.4 MPa) than one-seed juniper (P_{50} = −8.25 − −9.5 MPa; Hudson et al., 2018; Plaut et al., 2012). As measures of conductive capacity and xylem vulnerability to cavitation, we compared total xylem and phloem area, xylem and phloem conduit size, abundance of interconduit pits, interconduit pit diameter and width, and the latter of which has been related to cavitation vulnerability via inflection of the torus when aspirated (Hacke et al., 2004; Pittermann et al., 2010). To shed light on how hydraulically independent xylem and phloem tissues might be, we compare our results with the predictions of conduit size and increase in conduit abundance required for maintaining mass fluxes under drought (Figure S1).

2 | MATERIALS AND METHODS

2.1 | Sampling and imaging

Samples were collected at the Sevilleta precipitation manipulation experiment (Pangle et al., 2012; Plaut et al., 2012) in March 2013. The site is located in the Los Pinos—mountains within the Sevilleta National Wildlife Refuge in Socorro County, New Mexico (N 34°23′ 13″, W 106°31′29″). The experiment consisted of two precipitation manipulations (irrigation and drought) initiated in 2007 and two control treatments: ambient and control for drought structure (Pangle et al., 2012). For irrigation, ambient precipitation was enhanced by up to 42% each year and distributed using above-canopy sprinklers over the irrigation plots in three to six evenly distributed irrigation events during each growing season (April–September). For drought,

~50% of the surface area of the plots were covered with plastic troughs that redirected precipitation away from the plot. This resulted in ~45% reduction of available water from precipitation (for more details, see Pangle et al., 2012; Plaut et al., 2012; Dickman, McDowell, Sevanto, Pangle, & Pockman, 2014). We randomly selected two piñon pine and two one-seed juniper trees from ambient, irrigation, and drought treatments in treatment Block 1, the only replicate in which all trees were still alive after 5 years of treatment (Dickman et al., 2014). Two ~30- to 50-cm long branches from the south side of each tree were cut, immediately inserted in a PVC tube filled with water, and sealed with a stopper to maintain branch hydration during transport. All branches were placed in opaque plastic bags and transported in a plastic box insulated with expanded polystyrene to the Paul Scherrer Institute, Switzerland, for imaging. Branch transport from cutting to final measurement took a total of 5 days. Upon arrival, the cut ends were still submerged in water and all branches were functional, which was confirmed by measuring stomatal conductance under a growth light with a leaf porometer (SC-1 Decacon Devices, Pullman, WA, USA). At the Paul Scherrer Institute, we cut ~2 × 2 × 20mm (L × W × H) toothpick-like segments containing both xylem and phloem tissues including the cambial zone (Figure 1) from the middle of the branches with a razor blade under a light microscope. The segments were attached vertically to small sample holders using bee's wax. The wax was shaped to form a small bowl containing water to keep the sample moist during imaging.

The samples were imaged by phase contrast synchrotron radiation X-ray tomographic microscope at the TOMCAT beam line of Swiss Light Source, Paul Scherrer Institute, Villigen, Switzerland. The samples were placed inside an environmental chamber set to keep approximately 95% relative humidity at room temperature (for more detail, see Derome, Griffa, Koebel, & Carmeliet, 2011). During image acquisition, local tomography datasets were acquired on a specific region of interest (ROI) selected in the middle of the sample so that the xylem–phloem interface was visible (Figure 1). Due to the low X-ray attenuation coefficient of the samples, especially the phloem, the phase contrast imaging method was used. We used 15 keV energy, PCO.Edge 5.5 detector with 10× and 20× objectives leading to a pixel size of 0.65 or 0.35 μm, respectively. The sample was set 73 mm from the detector. The X-ray dosage is very low, resulting in no temperature change, nor any visual damage of the samples. Such damage during acquisition would have prevented reconstruction. We acquired 32 dark field and 100 flat field images for each sample to allow for image correction. For each sample measured with 10× magnification, we acquired 1,501 projections at equiangular positions over a total rotation angle range of 180° with 110 ms exposure. For samples measured with 20× magnification, the number of projections was 2,001. Each radiographic image consisted of 2,560 × 2,160 pixels leading to a window of view of ~1.6 × 1.4 or 0.9 × 0.8 mm^2, depending on the magnification. The 10× magnification (leading to 0.65 μm pixel size) was used initially for two control tree samples. This magnification allowed for analysis of conduit length, but pit structures remained obscure. To allow for pit size analysis, we used 20× magnification for all the other samples at the expense of conduit length analysis. The reconstruction procedure used phase retrieval with the Paganin algorithm. After reconstruction, the dataset for each sample consisted of 2,160 cross-sectional 2D slices of 2,560 × 2,560 pixels, 1 pixel apart in the axial direction. These images were then rendered to form 3D images of the samples using Avizo 3D (FEI, Hillsboro, OR, USA) and ImageJ (Schneider, Rasband, & Eliceiri, 2012) software.

For estimating the total phloem and xylem areas and xylem–phloem area ratios, we collected another set of branches from the same site. Sun exposed branches, 3–4 mm in diameter, and representing growth from the last 3–4 years, were collected from five drought and irrigation trees per species including all trees that were used for 3D imaging. The branches were sliced into thin segments close to the cut end and mounted on microscope slides using the free hand sectioning protocol of Taylor (1957). In this method, the samples are mounted moist, and their shape retained by the high moisture content. The samples were stained with cresyl violet to help identify the tissues and imaged with a compound light microscope (Zeiss AxioImager M1, Carl Zeiss MicroImaging, Gottingen, Germany) at 10× magnification at the University of New Mexico imaging laboratory. The leaf area supported by the xylem and phloem tissues of these branches was estimated based on stem diameter at the cut end of each sample using allometric equations for each treatment measured for these trees in the year prior to sample collection (Ms. Amanda Boutz, unpublished data).

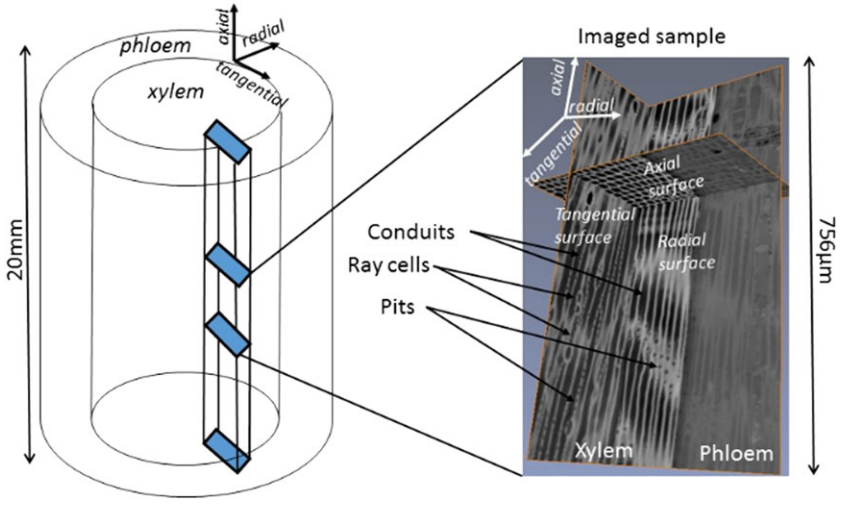

FIGURE 1 A schematic presentation of the samples imaged with X-ray tomography and the orientation of different planes in the samples. Our samples were matchstick-like segments cut at the xylem–phloem transition from branches of 3–5 years of age. The axial, tangential, and radial directions of the sample are indicated by the coordinates and the surfaces labelled with tissues and some anatomical features in an example of a 3D rendered image of a sample (on the right)

2.2 | Image analysis

All image analysis was completed using the visualization and analysis software Avizo 3D (FEI, Hillsboro, OR, USA) and ImageJ (Schneider et al., 2012). Total xylem and phloem areas were determined from the light microscopy images by tracing the xylem and phloem boundaries and using the ImageJ area measurement tool. Total tissue area included conduit lumens, cell walls, and possible ray cells and resin ducts located within the tissue but excluded the central pith. Typical of coniferous species (Schulz, 1990), the phloem of both species consisted almost exclusively of sieve elements, and therefore, this method gave a realistic estimate of conduit numbers. Total xylem and phloem areas were measured in two excisions from each branch, cut at least 1 cm apart to avoid pseudoreplication of the same conduits, and averaged.

2.3 | Xylem and phloem conduit size analysis

Xylem and phloem conduit sizes were measured from the 3D X-ray tomography images. In order to analyze a representative array of conduit diameters from the 3D renderings, three slices, namely, 400; 1,000; and 1,800 from within the 2,160 slices making one dataset, were taken. This allowed us to measure conduits at multiple points along their length, removing any bias among cell sizes from a single image. Single conduits appeared to be ~1 mm in length (determined from the images of the samples measured with 10× magnification), thus exceeding the length of most of our imaged samples (imaged at 20× magnification). To minimize the possible influence of pseudoreplication and human bias in selecting xylem conduits for analysis, we divided each growth ring of the xylem into 10 equal sections, two rows by five columns. A random number generator was then used to select one to two target conduits from within each section. Thus, a total of 10–20 xylem conduits were selected from each image, depending on the size of the image and the identifiability of the cells. Once each conduit was selected, the freehand selection tool in ImageJ was used to outline the target cell. The cell was designated as a ROI and added to the ROI Manager. Once all xylem conduits for an image were collected, the area of each cell was measured using the "analyze particle" function in ImageJ.

The phloem structure of both species closely resembled the anatomical organization of the xylem. The phloem consisted almost solely of sieve elements with companion cells embedded in the conduit wall (see also Schulz, 1990). In pine, easily identifiable large resin ducts were the main cell type in addition to sieve elements. In juniper, the sieve element rows were occasionally transversed by clusters of fibers with high contrast in our images (Figure 2). In both species ray cells continued from the xylem through the cambial zone to the phloem and could be easily identified from the 3D tomography images. Based on these observations and comparisons with Saderi, Pourtahmasi, Oladi, and Rathgeber (2013), Schweingruber et al. (2006), Alfieri and Evert (1973), and Abbe and Crafts (1939), phloem conduits were identified within the first approximately five cell layers from the cambium to ensure they were still living (Alfieri & Evert, 1973). All easily identifiable conduits within this five-cell layer section were selected and analyzed in the same way as xylem conduits.

2.4 | Pit abundance and size analysis

For analysis of pits, the 3D datasets of each sample produced by Avizo software were aligned with a global coordinate system, adjusted for brightness and contrast, and sliced in both the radial and tangential directions (see Figure 1) to produce three cross-sections in each direction. The cross-sections were obtained from both ends and the middle of the sample to avoid sampling the same conduits multiple times. Pit abundance was defined as the number of pits per cross-sectional area. This measure was selected because our samples did not cover the whole length of conduits, and therefore, the number of pits per conduit could not be calculated reliably. Each tangential surface slice was divided into six equal sections, three rows by two columns. A random number generator was used to select three of the six sections.

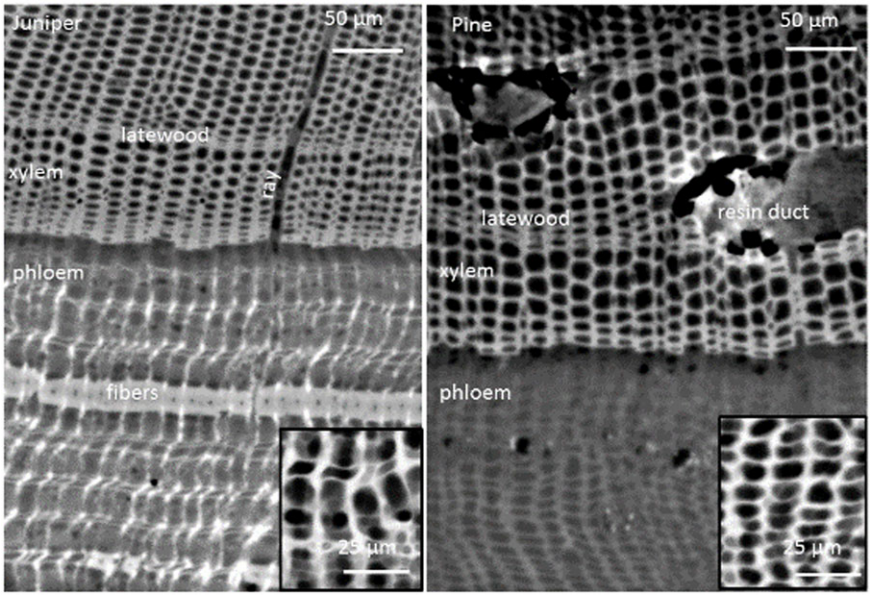

FIGURE 2 Axial views of irrigated one-seed juniper (left) and piñon pine (right) tissues at the xylem–phloem transition. In both images, xylem is the region of high contrast at the top of the image with less-structured phloem below. Two and three late-wood regions are clearly visible in one-seed juniper and piñon pine xylem, respectively. The newest growth ring (closest to the phloem boundary) is from 2012. In juniper, a ray from xylem to phloem is visible. In pine, two resin ducts are visible. Lighter areas are materials more interactive with X-rays (fibers, more lignified cell walls, and clusters of sugars). In juniper phloem, rows of fibers are common, and conduit walls in the radial direction are very thin (insert). In pine phloem, the structure is more uniform, although there still is a clear difference in radial and tangential cell wall thickness between xylem and phloem (insert) [Colour figure can be viewed at wileyonlinelibrary.com]

The total number of pits in each of these three sections was counted. This total was then divided by the area of the section calculated using the measurement tool in ImageJ. The number of pits for each of the three sections was then averaged to determine the mean number of pits per area of each slice. These averages were used in the statistical model as independent samples of the dependent variable. Tree identity was set as a random variable to avoid pseudoreplication issues stemming from the analysis of multiple images per tree (see Section 2.7).

Pit diameter, equivalent to membrane diameter in Hacke et al. (2004), was measured from radial and tangential cross-sections using Avizo software. Tangential surface cross-sections revealed pits that connect conduits in the tangential direction as small holes in the cell walls (Figure 1). Similarly, radial surface cross-sections showed pits that connect conduits in the radial direction as small openings in the cell wall. Pit size was measured by scanning through the cell wall in the 3D analysis mode of Avizo and counting the number of slides from the first visible opening of the pit until it closed. Pit size was then obtained by multiplying the number of slides by the image pixel size. This method allowed for faster and more reliable measurement of pit size for a large number of pits than measuring the diameter of the circular pit openings (Figure 1). Our image contrast and resolution was not sufficient for visualizing more detailed pit structures such as the size of the torus and margo.

To determine average pit size of each sample, we randomly selected 10 pits in each of the three slides. For tangential pits, we used only the 2012 growth ring. For radial pits, we measured pits at any growth ring because they occurred only in the latewood cell walls and were thus fewer (see Section 3). This procedure resulted in 10 to 40 pits analyzed per sample.

Pit width was defined as the length of the pit opening through the cell wall (representative of r_y in Hacke et al., 2004) and measured using the images identified above and the ImageJ measurement tool. Ten pits for which the full width was visible were randomly selected from each of the three image sections. Each measurement was treated as an independent measurement with no averaging in the statistical model.

2.5 | Xylem and phloem conduit abundance

To test the model predictions of Hölttä et al. (2009) on the ratio of xylem and phloem conduit abundance and tissue transport capacity, we combined the conduit size measurements from X-ray tomography with total xylem and phloem areas measured using light microscopy. The xylem-to-phloem conduit abundance ratio was calculated as

$$\frac{n_x}{n_p} = \frac{A_x}{a_x}\frac{a_p}{A_p} \quad (2)$$

where n_x and n_p are the number of xylem and phloem conduits, A_x and A_p the total areas of xylem and phloem tissue measured from light microscopy images, and a_x and a_p the average conduit areas of each tree measured from the X-ray tomography images. This approach takes into account the possible differences in xylem and phloem conduit sizes that were omitted in the model of Hölttä et al. (2009). Phloem and xylem tissue in this analysis consisted of all the cell types included in the region identified as phloem or xylem (Figure S2). In pine, the phloem was surrounded by a large layer of parenchyma cells identified as storage tissue and not included in phloem area.

2.6 | Error analysis

In the xylem, the conduits and other structures were generally easy to identify as a result of high contrast in the images, but in the phloem, this was more challenging (Figure 1). Error in conduit size and pit size due to difficulty in determining the exact boundary between lumen and cell wall was estimated by measuring the difference between conduit sizes in the control treatment samples when brightness and contrast were set for the smallest and largest possible conduit size, respectively. We estimated that the error in the calculated xylem conduit area was ~4%, and in the phloem, it was ~8%. Error in pit size measurements resulted from the pixel size and was ~9–11% for images taken with 20× magnification and 16–20% for images taken with 10× magnification.

2.7 | Statistical Analysis

To evaluate which predictors (species, treatment, and tissue) explained variation in xylem and phloem conduit size, pit abundance, and pit size, we first built the most general linear mixed effects model for the variable in question using the package lme4 (Bates, Maechler, Bolker, & Walker, 2015) in R or anovan in Matlab (version 7.11.1 Mathworks Inc., Natick, MA, USA). Based on the significance of the predicting variables and their interactions, we then simplified the model using stepwise multiple regression to determine the minimum adequate model. Species and treatment were used as fixed effects. The factor "individual tree" was set as a random effect, with image number nested in this factor when appropriate. This allowed for the absorption of noise due to natural variation between and within individuals. We used a Gaussian error structure and log-transformed data in order to comply with the assumptions therein when appropriate. The model fits were confirmed using QQ-plots and the significance determined using the χ^2 test. When random effects were insignificant in absorbing variation, the significance of the differences between treatments, tissues, and species were determined using Tukey–Kramer post hoc test with *F*-statistics and significance level set at $p < .05$. For xylem and phloem conduit, and pit size the random effects absorbed 25% and 13% of the variation, respectively, leaving the applicability of the Tukey test slightly questionable, but even in these cases, the Tukey-test results agreed with the significances obtained from the linear mixed model. For pit abundance, xylem-to-phloem area ratio and xylem-to-phloem conduit abundance ratio random effects absorbed <5% of the variation and application of Tukey test can be considered robust.

To test for correlations between structural parameters such as conduit size and pit size, we conducted linear regression analysis for each species separately. Significance of correlations was tested using *t* test. Medium significance was defined as $p < .05$ and high significance as $p < .01$. *T*-test was also used to test whether the xylem-to-phloem area and conduit abundance ratios differed significantly from 1.

3 | RESULTS

3.1 | Xylem and phloem area and conduit size

Compared with the xylem area, phloem area was larger in juniper, whereas xylem area was larger than phloem area in pine (Figure 3a). This difference was consistent between drought and irrigation treatments, and the actual area ratios were not influenced by the treatments. There were no statistically significant differences between species or treatments in xylem-to-phloem conduit abundance ratios (Figure 3b). All these ratios were considerably smaller than the ones predicted by the Hölttä et al. (2009) model in both species ranging from 0.9 (9:10) in irrigated juniper to 2.3 (23:10) in drought pine, which was the only value statistically significantly different from one. The difference in xylem-to-phloem area ratio was due to considerable differences in tissue type distribution between pine and juniper branch cross-sections (Figure S2). The xylem area was similar in both species, but juniper had considerably more phloem than pine. The pine phloem was only a narrow strip around the xylem separated from the bark layer by parenchyma cells and resin ducts. In juniper there was no layer separating the phloem from the bark. In juniper the branch cross-sections consisted of 35 ± 4% xylem and 18 ± 2% phloem, whereas in pine cross-sections were composed of 10 ± 5% xylem and 8 ± 5% phloem (no statistically significant differences between treatments). These tissues supported three to four times more downstream leaf area in juniper than in pine. Sample leaf area in the juniper irrigated treatment was 94.5 ± 0.5 cm^2 and in drought treatment 66.7 ± 0.5 cm^2, whereas in pine, the leaf areas for these treatments were 24.9 ± 0.7 cm^2 and 23.8 ± 0.6 cm^2, respectively.

Conduit size, as well as the conductive capacity in both Hagen–Poiseuille flow and the semipermeable scenarios depended significantly on the three-way interaction of species, treatment, and tissue (χ^2 = 6.8436, p = .0327), but there were few statistically significant differences between species, tissues, or treatments (Figure 4). In juniper, phloem conduits were larger than xylem conduits in the drought treatment, and their conductive capacity was twice of the conductive capacity of xylem conduits in the semipermeable conduit wall scenario (Figure 4b) and a five times the conductive capacity of xylem conduits in Hagen–Poiseulle flow (Figure 4c). Note that this comparison is somewhat arbitrary because we can expect flow in the xylem to follow the Hagen–Poiseuille equation, but in the phloem, it is possible that the conduit walls are semipermeable. In pine, phloem conduit size decreased progressively with increasing precipitation resulting in significantly smaller conduits and lower transport capacity in irrigation than in drought. In juniper, phloem conduit size did not respond to the treatments.

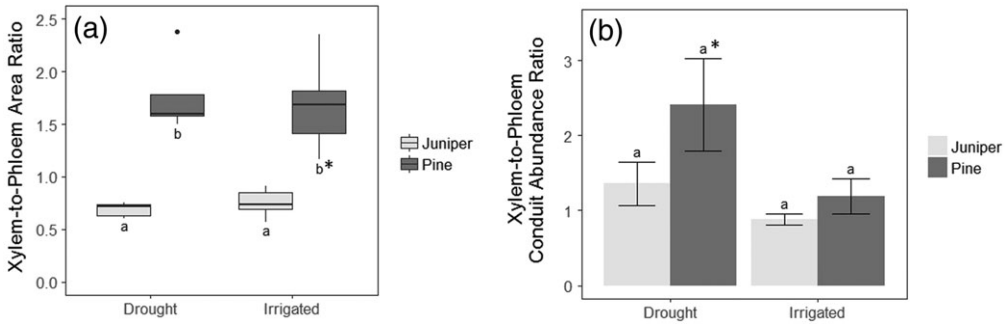

FIGURE 3 Average (a) xylem-to-phloem area and (b) conduit abundance ratio in piñon pine and one-seed juniper grown under drought and irrigation treatments. Different letters indicate statistically significant differences. In area, there is more phloem than xylem in juniper, whereas in pine, there is more xylem than phloem. Conduit abundance is higher in the xylem than in the phloem except in irrigated juniper. In panel (a), the middle line shows the median, the bottom and top of the box 25 and 75 percentiles. Values outside this range are plotted individually. The error bars in panel (b) indicate the maximum or interquantile range of the data. Different letters indicate statistically significant differences. Asterisk marks the values that are statistically significantly different from 1 (t test p < .05)

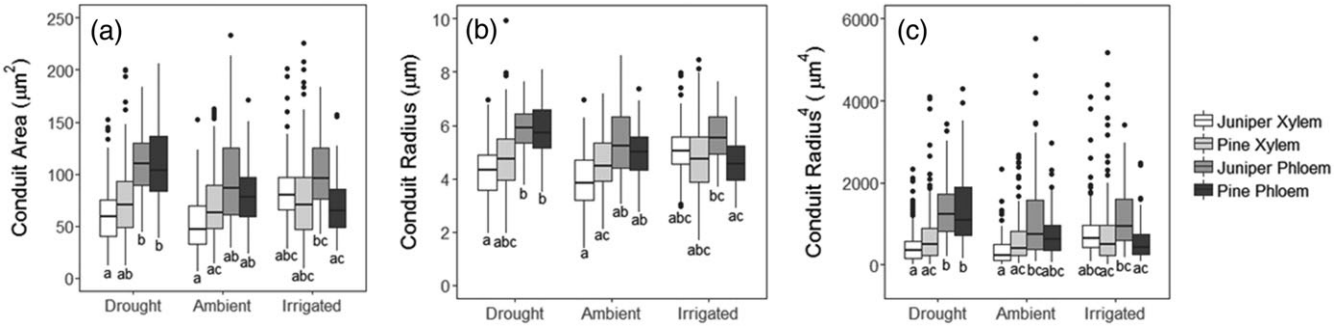

FIGURE 4 Average (a) conduit lumen area, (b) conduit radius, and (c) conduit radius to fourth power by treatment, tissue, and species. Conduit radius and conduit radius to fourth power represent conduit transport capacity in conduits with semipermeable and nonpermeable cell walls, respectively. The middle line shows the median, the bottom and top of the box 25 and 75 percentiles, and the error bars the maximum interquantile range of the data. Values outside this range are plotted individually. Different letters indicate statistically significant differences

Xylem conduits did not differ in size or transport capacity between species or treatments.

Though we did not quantify differences between treatments in growth ring formation, it was clear from the images that the growth rings were narrower in droughted trees than in irrigated trees (Figures 2 and 5). In droughted trees latewood regions typically consisted of only one or two cell layers with walls that were barely thicker than those found in the early wood, whereas in irrigated trees, the thickening of latewood cell walls was clear. In droughted pine, it was difficult to distinguish between growth rings using the axial images alone, but pits connecting conduits in the radial direction were found only at the cell walls of late wood and at the cambial zone. Their occurrence was thus used to help identify latewood and growth rings (Figure 5).

In both species, phloem cell walls in the tangential direction were thicker than the cell walls in radial direction (Figures 2, 5, and 6). In juniper the phloem conduits formed clusters of two conduits separated by a very thin cell wall in the radial direction, with a cell layer in between the clusters (Figure 6 insert), whereas in pine, the phloem conduits were surrounded by clearer cell walls. The thin cell wall between the phloem conduits in juniper could be a column of living cells dividing the conduit cluster into two or three compartments

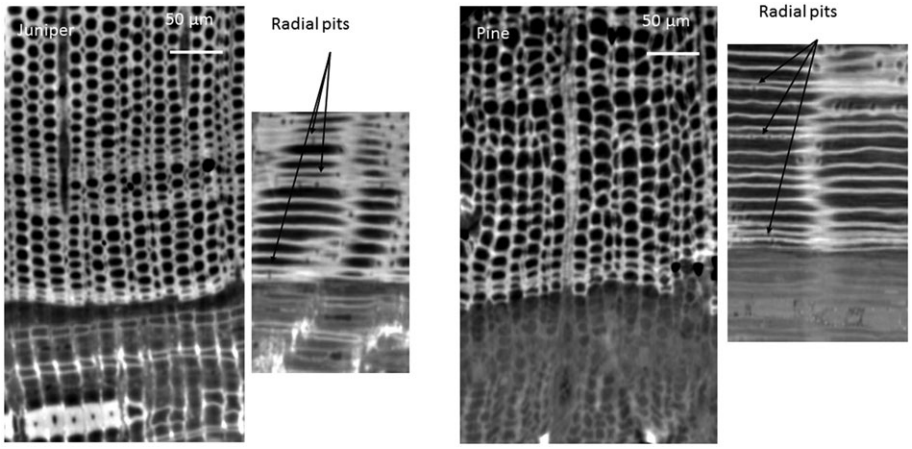

FIGURE 5 Axial and radial views of droughted juniper (left) and piñon pine (right) tissues at the xylem–phloem transition. Xylem is the region of high contrast at the top of the image with less-structured phloem below. Both samples have three growth rings. The rings are narrow and late wood consists of only a few cell layers in contrast to irrigated samples (Figure 2). Latewood regions are barely visible in pine and can be more easily identified in the tangential images by radial pits in the latewood cell walls. Radial pits were observed only in latewood tissue

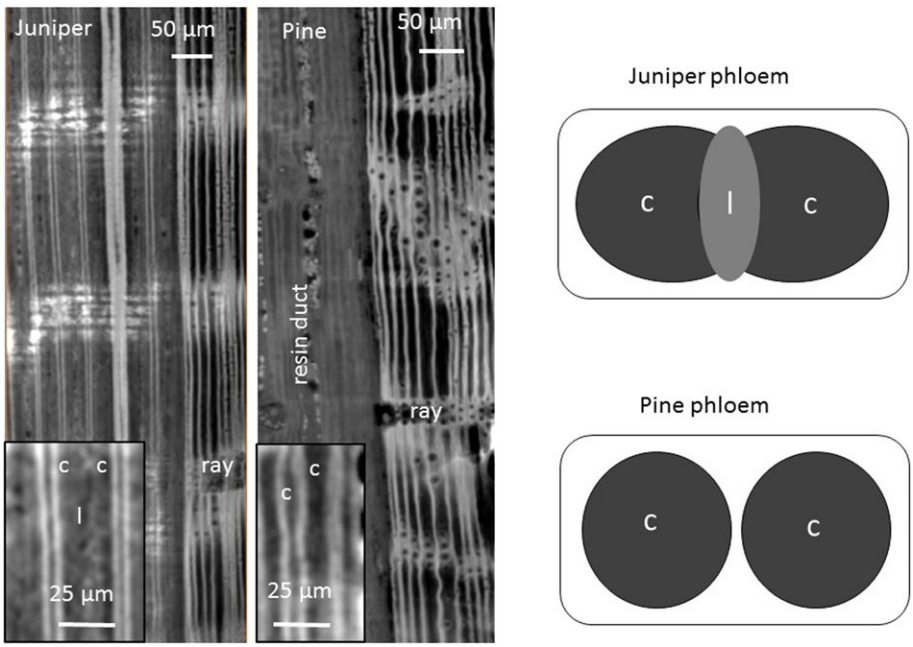

FIGURE 6 Radial surface images of irrigated juniper (left) and piñon pine (middle) at the xylem–phloem boundary and a schematic illustrations of phloem conduit structure in the axial view (right). In both images, xylem is on the right in the higher contrast area with clearer and denser cell walls. In juniper, the phloem appears to be missing every second cell wall. The "missing" wall forms a thin barrier between two conduits (c) that resembles a column of living cells (l; insert). In pine, the xylem structure repeats itself in the phloem. In the schematic illustrations, clusters of two conduits (c) of both species are presented. In juniper the two conduits are separated by a column of cells with thin, nonlignified walls (l), whereas in pine, the cell walls between conduits are more similar in every direction [Colour figure can be viewed at wileyonlinelibrary.com]

(Figure 6 and insert in Figure 2). In our analysis of conduit size, we treated the two conduits separated by the thin cell structure as individual conduits.

3.2 | Interconduit pits

Pits connecting xylem conduits in the tangential direction were very abundant at the conduit ends of both species (Figure 7). Radial pits were much less abundant than tangential pits and located only at late wood cell walls (Figure 5). Therefore, we only analyzed radial pits for pit size.

In the xylem, the abundance of tangential pits depended on species (χ^2 = 16.837, p < .0001) but not treatment (χ^2 = 2.474, p = .2903) or their interaction (χ^2_2 = 5.1834, p = .0748). Juniper trees had significantly more pits than pine trees (Figure 8a). In all species and treatments, tangential pits were larger than radial pits (F = 47.11 p < .001; Figure 8b), but the only significant difference in pit size was found between species when comparing irrigation treatment only. Irrigated junipers had significantly wider pits than irrigated pines (χ^2_1 = 6.0017, p = .0143; data not shown). In other treatments, there was no difference between species.

Tangential cell walls in the phloem of both species consisted of openings resembling xylem pits but lacking clear pit borders (Figure 7). These clusters of openings have been identified as sieve pore areas (Schulz, 1990). In pine, sieve pores seemed to be clearly clustered to distinct areas. In juniper, however, they were so abundant that the whole conduit wall seemed to be perforated by sieve pores making the phloem look more like an interconnected conduit network rather than consisting of individual, isolated conduits. In pine, phloem sieve pores were similar in size to tangential xylem pits and no statistically significant differences were found between treatments (data not shown). In the juniper phloem, the images were not clear enough for reliable analysis of sieve pore size.

To test for correlations between these structural parameters, we conducted simple regression analyses for each species. Generally, there were more significant correlations between structural traits in juniper than in pine, but the only highly significant correlation was found between the size of radial and tangential pits in pine (Table 1).

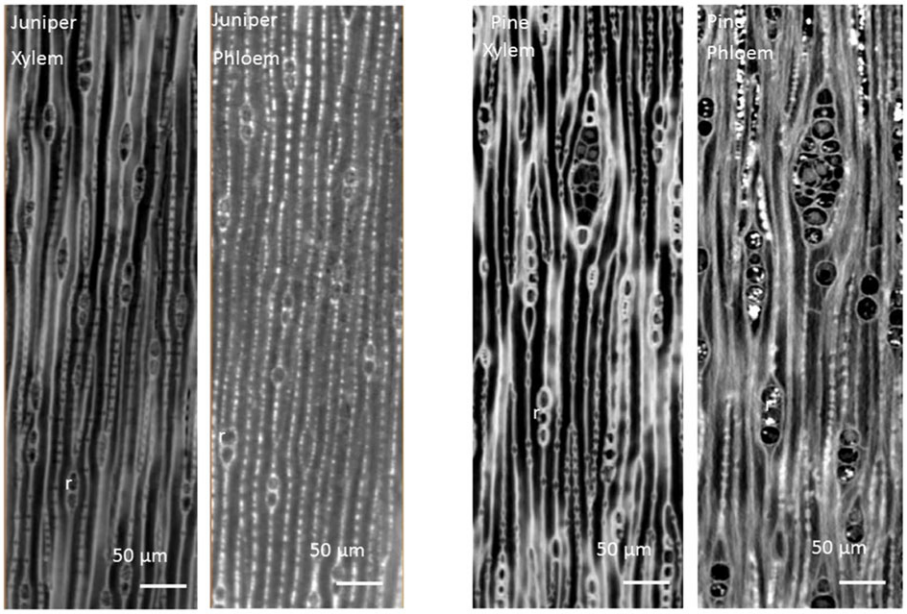

FIGURE 7 angential surface of juniper (left) and piñon pine (right) xylem and phloem. Ray cells (r) are visible as widenings in the cell walls, pits that allow flow in the tangential direction as small gaps in the cell walls. In juniper phloem the cell walls appear to be perforated with sieve pores throughout the sample while in the xylem, and in both tissues of pine, the interconduit connections are concentrated at conduit endings. There is much more dense material (possibly sugars) in the ray cells of pine than in juniper [Colour figure can be viewed at wileyonlinelibrary.com]

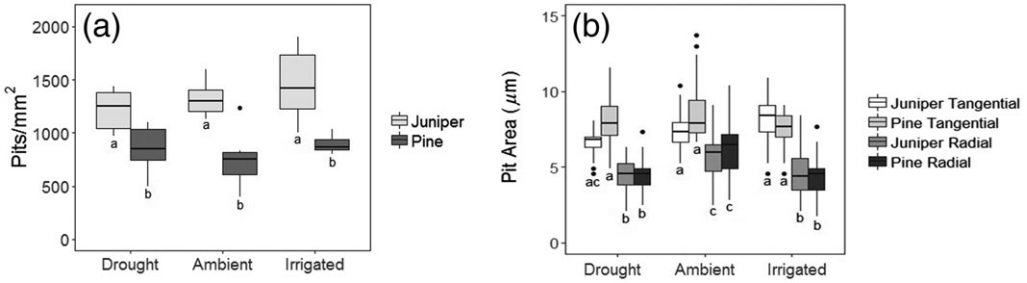

FIGURE 8 Xylem (a) pit abundance for tangential pits and (b) pit size for tangential and radial pits by species and treatment. The middle line shows the median, the bottom and top of the box 25 and 75 percentiles, and the error bars the maximum or interquantile range of the data. Values outside this range are plotted individually. Different letters indicate statistically significant differences

TABLE 1 Correlation coefficients between different anatomical properties for one-seed juniper and piñon pine

	Phloem conduit size	Pit abundance	Tangential pit size	Radial pit size
Xylem conduit size	**−0.1233** 0.1410	**0.6448*** 0.4257	**0.2356** 0.0889	**0.0230** 0.2225
Phloem conduit size	1	**0.3138** 0.1163	**−0.8479*** 0.4213	**−0.8212*** 0.2455
Tangential pit size	**−0.8479*** 0.4213	**−0.0640** 0.5814	1	**0.5675** 0.9731**
Radial pit size	**−0.8212*** 0.2455	**−0.2406** 0.5440	**0.5675** 0.9731**	1

Note. Significance of correlations was tested using *t* test. Medium significance ($p < .05$) is marked with *, highly significant ($p < .01$) with **. The perfect correlations of a variable with itself are marked with 1. Values for juniper are in bold.

In both species, radial pits were about half the size of tangential pits (Figure 9). The slopes were not significantly different between species. In juniper, phloem conduit size was inversely related to both tangential and radial pit size in the xylem suggesting that higher phloem conduit transport capacity could be linked with lower connectivity between conduits. On the other hand, pit abundance in juniper was positively correlated with xylem conduit size suggesting that larger xylem conduits have a higher pit density. In pine, there was no correlation between phloem conduit size and pit size or xylem conduit size and pit abundance, but the correlation between pit abundance and tangential pit size was almost significant. This suggests that in pine, there might be a tendency towards more pits resulting in smaller pits. In juniper, pit size and abundance were unrelated.

4 | DISCUSSION

Our anatomical analysis revealed two major differences between the desiccation-tolerant one-seed juniper and desiccation-avoiding piñon pine that were independent of precipitation treatments. One-seed juniper twigs had more phloem area compared with xylem area than piñon pine (Figure 3). Additionally, there were more tangential pits per xylem area in juniper than in pine (Figure 8). The findings on phloem area are in line with what would be expected based on the connection between stomatal closure point and hypothesized phloem transport limitations during drought. The more vulnerable piñon pine closes stomata at higher leaf water potentials than the less vulnerable one-seed juniper (Garcia-Forner et al., 2016; Plaut et al., 2012). To maintain phloem transport at low leaf water potential, juniper needs to invest in larger phloem tissue than pine (Hölttä et al., 2009; Sevanto, 2014). The pit abundance, however, contradicts what would be expected based on xylem vulnerability of these species (Figure 8). Based on higher vulnerability, and generally higher sap flow rates in pine than in juniper (Plaut et al., 2012), we expected pine to show higher pit abundance than juniper. Our results suggest that differences in pit abundance, size, or width or in conduit size are not responsible for the difference in xylem vulnerability to embolism between these species (Figures 4 and 8). Differences in vulnerability of the torus–margo system, however, are possible. If pine torus contained, for example, more plasmodesmal pores than juniper torus did, higher vulnerability could be expected (Jansen et al., 2012) even independent of pit abundance.

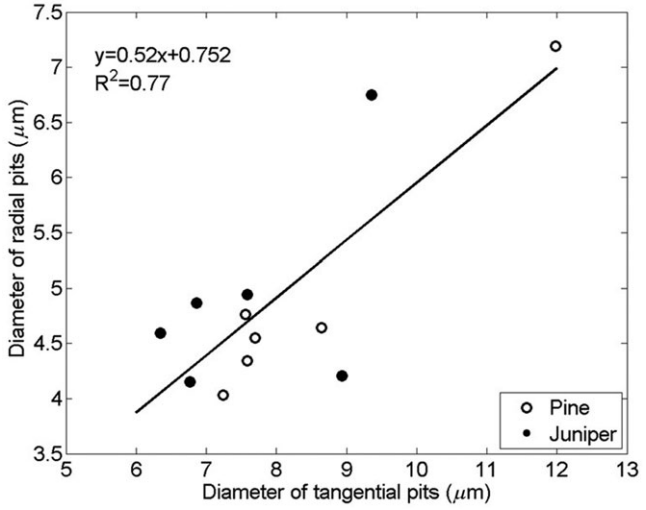

FIGURE 9 Radial and tangential pit size are positively correlated. In both species, radial pits were roughly half the size of tangential pits. The relationship was stronger in pine than in juniper (Table 1), but the slopes did not differ significantly between species

The larger phloem area and relative conduit abundance in one-seed juniper than in piñon pine agree with the general trend suggested by Equation 1 (Figure S1) and Hölttä et al. (2009) of low stomatal closure point generating a need for more phloem to maintain transport capacity. The conduit abundance ratios, however, were considerably lower than would have been expected showing larger than predicted phloem area in both species. (Figure 3b). The Hölttä et al. (2009) study assumed similar conduit size both in the xylem and the phloem, but our lower conduit abundance ratios could not be explained by the observed differences in conduit sizes between these tissues (Figure 4). The large amount of phloem conduits compared with xylem conduits in both species might be due to differences in tissue distributions between young twigs and the main stem of trees. In older branches and tree parts, the amount of xylem tends to increase faster than the amount of phloem (Jyske & Hölttä, 2015), and the Hölttä et al. (2009) model considers tree stems rather than young twigs. Interestingly, the difference in phloem area fraction matched the difference in supported downstream leaf area between species, though no difference in phloem area between juniper treatments was found despite a large difference in leaf area between drought and irrigation twigs.

The low xylem-to-phloem conduit abundance could also be an indication of the different transport mechanisms in these two tissues. The xylem transport capacity could be higher compared with the phloem transport capacity even if the conduit abundance is similar

because the flow is driven by different pressure gradients, and conduit size affects the hydraulic resistance differently. A true comparison of relative efficiency of transport in conduits with nonpermeable and semipermeable walls is difficult because the pressure gradients driving the flow are not comparable. In nonpermeable conduits, the pressure gradient that drives the flow is a vertical gradient between the two ends of the conduits, whereas in conduits with semipermeable walls, a local vertical gradient that drives the flow is generated by a horizontal osmotic pressure gradient between conduits and their surroundings (Phillips & Dungan, 1993, Sevanto, 2014). It is also possible that the phloem in piñon pine and one-seed juniper operate differently. We observed an abundance of sieve pores in juniper phloem, whereas the structure of piñon pine phloem suggested greater similarity to the xylem transport system (Figure 7). Furthermore, in one-seed juniper, the phloem conduits formed clusters of two conduits separated by a column of cells that could have flexible walls and contain sugars (Figure 6). Even though we report no difference in phloem conduit size between pine and juniper, these structural differences might lead to differences in transport capacity that are not explained completely by the comparison of transport capacity of conduits with semipermeable and nonpermeable walls. The flexible cell walls in juniper could influence the pressure development in the conduits, and the cells in the middle could induce loading and unloading of sugars described by the phloem relay scenario (Hölttä et al., 2009; Thompson & Holbrook, 2003). The operation of the clusters of two conduits might be better described as one unit rather than two separate conduits as was done in this study. Therefore, further investigation of the hydraulics of such systems is needed for robust conclusions of phloem adaptations to precipitation treatments in juniper and comparisons of phloem transport capacity between piñon pine and one-seed juniper.

Interestingly, our results suggest that structural adaptation to precipitation treatments was not very strong in these species. The only clear treatment effects were the difference in xylem and phloem conduit size in the drought treatment for both species, the increase in pit width with irrigation in juniper, and the increase in phloem conduit size with decreasing precipitation in piñon pine (Figure 4). The increased difference in xylem and phloem conduit size in drought treatment compared with other treatments was due to slightly increased phloem conduit size in piñon pine and slightly decreased xylem conduit size in one-seed juniper. This suggests that contrary to our hypothesis piñon pine rather than one-seed juniper seems to adapt to precipitation changes by changing phloem conduit size. Juniper's adaptation, on the other hand, was focused on the xylem, possibly making it even less vulnerable by reducing conduit size, although no treatment effect in xylem vulnerability have been reported on trees of this experiment (Hudson et al., 2018; Plaut et al., 2012). Another explanation for this adaptation pattern could be that juniper has already optimized its phloem structure for transport capacity in any conditions it is likely to encounter, and therefore, no change was needed to adapt to drought treatment, but more moist conditions allowed it to invest in increasing xylem transport capacity and maintaining higher leaf area in the irrigation treatment. Similarly, pine could have optimized xylem conduit size for transport in its realm but may have benefitted from increased phloem conduit size under drought conditions, due to lower interconduit connectivity via sieve pores than in juniper. In conduits with nonpermeable walls even a small change in conduit diameter has a large effect on flow resistance (Figure S1). The observed changes of ~1–2 μm (33%) between irrigated and droughted trees (Figure 4) would mean a three-fold increase in conductivity (Hagen–Poiseuille equation) in pine. This change in conductivity would translate to an increase of about 1 MPa in the osmotic potential that could be tolerated without viscosity-induced decline in mass flux when a plant operates at xylem water potentials >−4 MPa (Figure S1). Below −4 MPa xylem water potentials, the size of conduits has to increase much more rapidly to achieve similar gains in tolerable osmotic potentials. This might explain why juniper phloem structure differs from xylem structure more than pine phloem does. Interestingly, there was no correlation between xylem and phloem conduit size in either species, which suggests that these slight adaptations are tissue specific and independent of each other, even if the overall cellular structure continues from one tissue to the other through the cambium (Figure 9).

The speculations on piñon pine phloem operating like a system of independent conduits with nonpermeable walls are contrary to our hypotheses and those suggested by Sevanto (2014) based on the theories of ease of phloem transport and turgor loss during drought. These hypotheses suggest that desiccation-tolerant plants would benefit from less permeable conduit walls to reduce the influence of changes in xylem water potential on phloem transport. Desiccation-avoiding plants, on the other hand, could have high hydraulic conductivity between the xylem and the phloem, because they control the declining xylem water potential by early stomatal closure. These hypotheses are supported by our observation of large storage tissue surrounding the phloem in piñon pine (Figure S2) and the branch-scale observations of Malone et al. (2016), which suggested higher hydraulic conductivity in the radial direction in pine than in juniper. These hypotheses and all our findings, however, could still fit together if the turgor loss in pine phloem (Sevanto et al., 2014) was facilitated by turgor loss in the storage tissue rather than in phloem conduits, and the highest resistance to radial water flux in juniper was at the cambial zone rather than between phloem conduits. More detailed information on the anatomy and function of different components of the phloem tissue is thus needed to understand the vulnerability of phloem transport in these species. One intriguing aspect of the hydraulic connection between the xylem and the phloem are radial pits found in both species only in latewood and across the cambial zone (Figure 5). Even though small and sparse, these pits facilitate a direct hydraulic connection between these tissues allowing water to move from one growth ring to another and from the xylem to the phloem even if the conduits themselves have nonpermeable walls.

It is also intriguing that in juniper pit size in both tangential and radial directions was inversely correlated with phloem conduit size and not correlated with xylem conduit size. In line with the model results of Hölttä et al. (2009), this could be interpreted as higher phloem transport capacity requiring lower hydraulic conductivity in the xylem and between the xylem and the phloem. Whether the hydraulic connection between the xylem and the phloem is the root cause of small pit sizes, and small tangential pits just follow from genetic coordination of radial and tangential pit size, remains to be shown. It is equally possible that small tangential pits could be

triggered by the need to decrease xylem vulnerability to embolism, and small radial pit size and large phloem conduit size would be simply responses to this. Although it was not statistically significant in our data set, there was a trend in juniper towards larger tangential pits with increasing precipitation (Figure 8), which supports the latter interpretation. All in all, our results suggest that high hydraulic transport capacity can be obtained via various anatomical adaptations, and some coordination in tissue anatomy occurs in an unexpected manner.

5 | CONCLUSIONS

We tested hypotheses presented in the literature about how different stomatal closure points would be reflected in xylem and phloem anatomy of desiccation-avoiding and desiccation-tolerant plants using three-dimensional X-ray tomography and light microscopy imaging. Our results support the hypothesis that desiccation-tolerant species need more conductive phloem tissue than desiccation-avoiding species to maintain phloem transport at low tissue water potentials. An increase in phloem transport capacity, however, is not necessarily obtained only by increasing phloem tissue or conduit size. The contrast in juniper and pine phloem anatomy and in anatomical response to decreased precipitation suggests that higher transport capacity can be obtained via various anatomical features that support good hydraulic connection between phloem sieve elements.

ACKNOWLEDGMENTS

We want to thank Dr. David Habitur from PSI for technical help in x-ray imaging, Mr. Kent Coombs and Ms. Jamie Resnick for analysis of xylem versus phloem area data, and Ms. Amanda Boutz for the leaf area estimates. This study was financed by Los Alamos National Laboratory LDRD program projects number 20130442ER and 20160373ER, the Sevilleta LTER program (NSF DEB-0620482), Department of Energy's Office of Science (BER), and the UNM Sevilleta Field Station, and Paul Scherrer Institute award 20120914. The authors have no conflict of interest to declare.

ORCID

Sanna Sevanto http://orcid.org/0000-0001-9127-5285
L. Turin Dickman http://orcid.org/0000-0003-3876-7058
Patrick J. Hudson http://orcid.org/0000-0001-7759-2321

REFERENCES

Abbe, L. B., & Crafts, A. S. (1939). Phloem of white pine and other coniferous species. *Botanical Gazette*, *100*, 695–722.

Alfieri, F. J., & Evert, R. F. (1973). Structure and seasonal development of the secondary phloem in the pinaceae. *Botanical Gazette*, *134*, 17–25.

Bates, D., Maechler, M., Bolker, B., & Walker, S. (2015). Fitting linear mixed-effects models using lme4. *Journal of Statistical Software*, *67*, 1–48.

Berninger, F., Mäkelä, A., & Hari, P. (1996). Optimal control of gas exchange during drought: Empirical evidence. *Annals of Botany*, *77*, 469–476.

Bird, R. B., Stweart, W. E., & Lightfoot, E. N. (2002). *Transport phenomena* (2nd ed.). (pp. 40–113). New York: John Wiley & Sons.

Brodersen, C., Jansen, S., Choat, B., Rico, C., & Pittermann, J. (2014). Cavitation resistance in seedless vascular plants: The structure and function of interconduit pit membranes. *Plant Physiology*, *165*, 895–904.

Brodersen, C. G. (2015). Finding support for theoretical tradeoffs in xylem structure and function. *New Phytologist*, *209*, 8–10.

Brodribb, T. J. (2009). Xylem hydraulic physiology: The functional backbone of terrestrial plant productivity. *Plant Science*, *177*, 242–251.

Brodribb, T. J., & Hill, R. S. (1999). The importance of xylem constraints in the distribution of conifer species. *New Phytologist*, *143*, 365–372.

Brodribb, T. J., Holbrook, N. M., Edwards, E. J., & Gutierrez, M. V. (2003). Relations between stomatal closure, leaf turgor and xylem vulnerability in eight tropical dry forest trees. *Plant, Cell and Environment*, *26*, 443–450.

Cai, J., & Tyree, M. T. (2010). The impact of vessel size on vulnerability curves: Data and models for within-species variability in saplings of aspen, *Populus tremuloides* Michx. *Plant, Cell and Environment*, *33*, 1059–1069.

Choat, B., Ball, M., Luly, J., & Holtum, J. (2003). Pit membrane porosity and water stress-induced cavitation in four co-existing dry rainforest tree species. *Plant Physiology*, *131*, 41–48.

Choat, B., Jansen, S., Zwieniecki, M. A., Smets, E., & Holbrook, N. M. (2004). Changes in pit membrane porosity due to deflection and stretching: The role of vestured pits. *Journal of Experimental Botany*, *55*, 1569–1575.

Christman, M. A., Sperry, J. S., & Adler, F. R. (2009). Testing the 'rare pit' hypothesis for xylem cavitation resistance in three species of *Acer*. *New Phytologist*, *182*, 664–674.

Cochard, H., Breda, N., & Granier, A. (1996). Whole tree hydraulic conductance and water loss regulation in *Quercus* during drought. Evidence for stomatal control of embolism? *Annals of Forest Science*, *53*, 197–206.

Cochard, H., Hölttä, T., Herbette, S., Delzon, S., & Mencuccini, M. (2009). New insights into mechanisms of water-stress-induced cavitation in conifers. *Plant Physiology*, *151*, 949–954.

Cowan, I. R., & Farquhar, G. D. (1977). Stomatal function in relation to leaf metabolism and environment. *Soc. Exp. Biol. Symp.*, *31*, 471–505.

Delzon, S., Douthe, C., Sala, A., & Cochard, H. (2010). Mechanism of water-stress induced cavitation in conifers: Bordered pit structure and function support the hypothesis of seal capillary-seeding. *Plant, Cell and Environment*, *33*, 2101–2111.

Derome, D., Griffa, M., Koebel, M., & Carmeliet, J. (2011). Hysteretic swelling of wood at cellular scale probed by phase contrast X-ray tomography. *Journal of Structural Biology*, *173*, 180–190.

Dickman, L. T., McDowell, N. G., Sevanto, S., Pangle, R. E., & Pockman, W. T. (2014). Carbohydrate dynamics and mortality in a piñon-juniper woodland under three future precipitation scenarios. *Plant, Cell and Environment*, *38*, 729–739.

Domec, J. C., & Gartner, B. L. (2002). Age- and position-related changes in hydraulic versus mechanical dysfunction of xylem: Inferring the design criteria for Douglas-fir wood structure. *Tree Physiology*, *22*, 91–104.

Fucaloro, A. F., Pu, Y., Cha, K., Williams, A., & Conrad, K. (2007). Partial molar volumes and refractions of aqueous solutions of fructose, glucose mannose and sucrose at 15.00, 20.00, and 25.00°C. *Journal of Solution Chemistry*, *36*, 61–80.

Garcia-Forner, N., Adams, H. D., Sevanto, S., Collins, A. D., Dickman, L. T., Hudson, P. J., … McDowell, N. G. (2016). Responses of two semiarid confer tree species to reduced precipitation and warming reveal new perspectives for stomatal regulation. *Plant, Cell and Environment*, *39*, 38–49.

Gleason, S. M., Westoby, M., Jansen, S., Choat, B., Hacke, U. G., Pratt, R. B., … Zanne, A. E. (2015). Weal tradeoff between xylem safety and xylem-specific hydraulic efficiency across the world's woody plant species. *New Phytologist*, *209*, 123–136.

Hacke, U. G., Sperry, J. S., & Pittermann, J. (2004). Analysis of circular bordered pit function II. Gymnosperm tracheids with torus-margo pit membranes. *American Journal of Botany*, *91*, 386–400.

Hölttä, T., Mencuccini, M., & Nikinmaa, E. (2009). Linking phloem function to structure: Analysis with a coupled xylem-phloem transport model. *Journal of Theoretical Biology*, *259*, 325–337.

Hudson, P. J., Limousin, J. M., Krofcheck, D. J., Boutz, A. L., Pangle, R. E., Gehres, N., … Pockman, W. T. (2018). Impacts of long-term precipitation manipulation on hydraulic architecture and xylem anatomy of piñon and juniper in Southwest USA. *Plant, Cell and Environment*, *41*, 421–435. https://doi.org/10.1111/pce.13109

Irvine, J., & Grace, J. (1997). Continuous measurements of water tensions in the xylem of trees based on the elastic properties of wood. *Planta*, *202*, 455–461.

Jansen, S., Lamy, J. B., Burlett, R., Cochard, H., Gasson, P., & Delzon, S. (2012). Plasmodesmatal pores in the torus of bordered pit membranes affect cavitation resistance of conifer xylem. *Plant, Cell and Environment*, *35*, 1109–1120.

Jyske, T., & Hölttä, T. (2015). Comparison of phloem and xylem hydraulic architecture in *Picea abies* stems. *New Phytologist*, *205*, 102–115.

Katul, G., Manzoni, S., Palmroth, S., & Oren, R. (2010). Stomatal Optimization theory to describe the effects of atmospheric CO2 on leaf photosynthesis and transpiration. *Annals of Botany*, *105*, 431–442.

Kim, H. K., Park, J., & Hwang, I. (2014). Investigating water transport through the xylem network in vascular plants. *Journal of Experimental Botany*, *65*, 1895–1904.

Laur, J., & Hacke, U. G. (2014). Exploring *Picea glauca* aquaporins in the context of needle water uptake and refilling. *New Phytologist*, *203*, 388–400.

Limousin, J.-M., Bickford, C. P., Dickman, L. T., Pangle, R. E., Hudson, P. J., Boutz, A. L., … McDowell, N. G. (2013). Regulation and acclimation of leaf gas exchange in a piñon-juniper woodland exposed to three different precipitation regimes. *Plant, Cell and Environment*, *36*, 1812–1825.

LoGullo, M. A., Salleo, S., Piaceri, E. C., & Rosso, R. (1995). Relations between vulnerability to xylem embolism and xylem conduit dimensions in young trees of *Quercus cerris*. *Plant and Cell Physiology*, *18*, 661–669.

Malone, M. W., Yoder, J., Hunter, J. F., Espy, M. A., Dickman, L. T., Nelson, R. O., … Sevanto, S. (2016). In vivo observation of tree drought response with low-field NMR and neutron imaging. *Frontiers in Plant Science*, *7*. https://doi.org/10.3389/fpls.2016.00564

Manzoni, S., Vico, G., Katul, G., Palmroth, S., Jackson, R. B., & Porporato, A. (2013). Hydraulic limits on maximum plant transpiration and the emergence of the safety-efficiency trade-off. *New Phytologist*, *198*, 169–178.

Martinez-Vilalta, J., Prat, E., Oliveras, I., & Pinol, J. (2002). Xylem hydraulic properties of roots and stems of nine Mediterranean woody species. *Oecologia*, *133*, 19–29.

McDowell, N. G., Pockman, W. T., Allen, C. D., Breshears, D. D., Cobb, N., Kolb, T., … Yepez, E. A. (2008). Mechanisms of plant survival and mortality during drought: Why do some plants survive while others succumb to drought? *New Phytologist*, *178*, 719–739.

McDowell, N. G., & Sevanto, S. (2010). The mechanisms of carbon starvation: How, when, or does it even occur at all? *New Phytologist*, *186*, 264–266.

Meinzer, F. C. (2002). Co-ordination of vapor and liquid phase water transport properties in plants. *Plant, Cell and Environment*, *25*, 265–274.

Meinzer, F. C., Johnson, D. M., Lachenbruch, B., McCulloh, K. A., & Woodruff, D. R. (2009). Xylem hydraulic safety margins in woody plants: Coordination of stomatal control of xylem tension with hydraulic capacitance. *Functional Ecology*, *23*, 922–930.

Morison K.R. (2002) Viscosity equations for sucrose solutions: Old and new 2002. In: *Proceedings of the Nineth APCChE Congress and CHEMECA 2002*, Paper # 984.

Nardini, A., & Salleo, S. (2000). Limitation of stomatal conductance by hydraulic traits: Sensing or preventing xylem cavitation? *Trees*, *15*, 14–24.

Nikinmaa, E., Hölttä, T., Hari, P., Kolari, P., Mäkelä, A., Sevanto, S., & Vesala, T. (2013). Assimilate transport in phloem sets conditions for leaf gas exchange. *Plant, Cell and Environment*, *36*, 655–669.

Pangle, R. E., Hill, J. P., Plaut, J. A., Yepez, E. A., Elliot, J. R., Gehres, N., … Pockman, W. T. (2012). Methodology and performance of a rainfall manipulation experiment in a piñon–juniper woodland. *Ecosphere*, *3*, 28.

Pangle, R. E., Limousin, J. M., Plaut, J. A., Yepez, E. A., Hudson, P. J., Boutz, A. L., … McDowell, N. G. (2015). Prolonged experimental drought reduces plant hydraulic conductance and transpiration and increases mortality in a piñon-juniper woodland. *Ecology and Evolution*, *5*, 1618–1638.

Phillips, R. J., & Dungan, S. R. (1993). Asymptotic analysis of flow in sieve tubes with semi-permeable walls. *Journal of Theoretical Biology*, *162*, 465–485.

Pittermann, J., Choat, B., Jansen, S., Stuart, S. A., Lynn, L., & Dawson, T. E. (2010). The relationship between xylem safety and hydraulic efficiency in the Cupressaceae: The evolution of pit membrane form and function. *Plant Physiology*, *153*, 1919–1931.

Pittermann, J., Sperry, J. S., Hacke, U. G., Wheeler, J. K., & Sikkema, E. H. (2006). Inter-tracheid pitting and the hydraulic efficiency of conifer wood: The role of tracheid allometry and cavitation protection. *American Journal of Botany*, *93*, 1265–1273.

Plaut, J. A., Yepez, E. A., Hill, J., Pangle, R., Sperry, J. S., Pockman, W. T., & McDowell, N. G. (2012). Hydraulic limits preceding mortality in a piñon-juniper woodland under experimental drought. *Plant, Cell and Environment*, *35*, 1601–1617.

Quero, J. L., Sterck, F. J., Martinez-Vilalta, J., & Villar, R. (2011). Water-use strategies of six co-existing Mediterranean woody species during a summer drought. *Oecologia*, *166*, 45–57.

Saderi, S. M., Pourtahmasi, K., Oladi, R., & Rathgeber, C. B. K. (2013). Wood formation in *Juniperus excelsa* ssp. polycarpos in the high mountains of north-east Iran. *Journal of Tropical Forest Science*, *25*, 421–428.

Sala, A., Piper, F., & Hoch, G. (2010). Physiological mechanisms of drought induced tree mortality are far from being resolved. *New Phytologist*, *186*, 274–281.

Savage, J. A., Clearwater, M. J., Haines, D. F., Klein, T., Mencuccini, M., Sevanto, S., … Zhang, C. (2016). Allocation, stress tolerance and carbon transport in plants: How does phloem physiology affect plant ecology? *Plant, Cell and Environment*, *39*, 709–725.

Schneider, C. A., Rasband, W. S., & Eliceiri, K. W. (2012). NIH Image to ImageJ: 25 years of image analysis. *Nature methods*, *9*, 671–675. PMID 22930834

Schulz, A. (1990). Conifers. In H. D. Behnke & R. D. Sjolund (Eds.), *Sieve elements* (pp. 63–88). Berlin Heidelberg New York: Springer.

Schweingruber, F. H., Borner, A., & Schultze, E. D. (2006). *Atlas of woody plant stems: Evolution, structure, and environmental modifications*. (p. 227). Berlin: Springer.

Scoffoni, C., Albuquerque, C., Brodersen, C. R., Townes, S., John, G. P., Cochard, H., … Sack, L. (2017). Leaf vein xylem conduit diameter influences susceptibility to embolism and hydraulic decline. *New Phytologist*, *213*, 1076–1092.

Sevanto, S. (2014). Phloem transport and drought. *Journal of Experimental Botany*, *65*, 1751–1759.

Sevanto, S., Holbrook, N. M., & Ball, M. C. (2012). Freeze/thaw-induced embolism: probability of critical bubble formation depends on speed of ice formation. *Frontiers in Plant Biophysics and Modeling*, *3*, 1–12.

Sevanto, S., Hölttä, T., Markkanen, T., Perämäki, M., Nikinmaa, E., & Vesala, T. (2005). Relationships between diurnal diameter variations and environmental factors in Scots pine. *Boreal Environment Research*, *10*, 447–458.

Sevanto, S., McDowell, N. G., Dickman, L. T., Pangle, R., & Pockman, W. T. (2014). How do trees die? A test of the hydraulic failure and carbon starvation hypotheses. *Plant, Cell and Environment*, *37*, 153–161.

Smith, M. S., Fridley, J. D., Yin, J., & Bauerle, T. L. (2013). Contrasting xylem vessel constraints on hydraulic conductivity between native and non-native woody understory species. *Frontiers in Plant Science*, *4*, 486.

Sperry, J. S. (1986). Relationship of xylem embolism to xylem pressure potential, stomatal closure and shoot morphology in the palm *Rhapis excelsa*. *Plant Physiology*, *80*, 110–116.

Sperry, J. S. (2000). Hydraulic constraints on plant gas exchange. *Agricultural and Forest Meterology*, *104*(1), 13–23.

Sperry, J. S., & Pockman, W. T. (1993). Limitation of transpiration by hydraulic conductance and xylem cavitation in. *Betula occidentalis*. *Plant, Cell and Environment*, *16*, 279–287.

Sperry, J. S., Wang, Y., Wolfe, B. T., Mackay, D. S., Anderegg, W. R. L., McDowell, N. G., & Pockman, W. T. (2016). Pragmatic hydraulic theory predicts stomatal responses to climatic water deficits. *New Phytologist*, *212*, 577–589.

Tardieu, F., & Simonneau, T. (1998). Variability of species among stomatal control under fluctuating soil water status and evaporative demand: Modeling isohydric and anisohydric behaviours. *Journal of Experimental Botany*, *49*, 419–432.

Taylor, E. C. (1957). Freehand sectioning of moss leaves and stems. *The Bryologist*, *60*, 17–20.

Thompson, M. W., & Holbrook, N. M. (2003). Scaling phloem transport: Water potential equilibrium and osmoregulatory flow. *Plant, Cell and Environment*, *26*, 1561–1577.

Tyree, M. T., & Sperry, J. S. (1989). Vulnerability of xylem to cavitation and embolism. *Annual Review of Plant Physiology*, *40*, 19–38.

Wheeler, J. K., Sperry, J. S., Hacke, U. G., & Hoang, N. (2005). Inter-vessel pitting and cavitation in woody rosaceae and other vesselled plants: A basis for a safety vs. Efficiency trade-off in xylem transport. *Plant, Cell & Environment*, *28*, 800–812.

SUPPORTING INFORMATION

Additional Supporting Information may be found online in the supporting information tab for this article.

Figure S1: Increase required in phloem conduit diameter (a), and number of phloem conduits (b) to maintain mass flux unchanged with increasing osmotic potential. The conduit diameter ratio was calculated by combining the Hagen-Poiseuille equation with the van't Hoff equation and the semi-empirical equation of Morrison (2002) for viscosity increase as a response to increasing sucrose concentration.

Figure S2. Cross sections of young branches of pinon pine (left) and one-seed juniper (right) stained with cresyl violet to show the anatomical structures. In both species, the star-like structure in the middle is the pith (p), the surrounding tissue is the xylem (x), and the tissue around the xylem is the phloem (ph). In juniper, the phloem extends almost to the bark, but in pine there is a broad band of tissue consisting of parenchyma cells and resin ducts (r) between the phloem and the bark, which is labelled here with (s) to suggest its function as a sugar storage tissue.

How to cite this article: Sevanto S, Ryan M, Dickman LT, et al. Is desiccation tolerance and avoidance reflected in xylem and phloem anatomy of two coexisting arid-zone coniferous trees? *Plant Cell Environ*. 2018;41:1551–1564. https://doi.org/10.1111/pce.13198